

Autophagy enhances hepatocellular carcinoma progression by activation of mitochondrial β -oxidation

戸島, 剛男

<https://doi.org/10.15017/1441068>

出版情報 : 九州大学, 2013, 博士 (医学), 課程博士
バージョン :
権利関係 : 全文ファイル公表済

Autophagy Enhances Hepatocellular Carcinoma Progression by Activation of Mitochondrial β -oxidation

Takeo Toshima, MD; Ken Shirabe, MD, PhD; Yoshihiro Matsumoto, MD; Shohei Yoshiya, MD; Toru Ikegami, MD, PhD; Tomoharu Yoshizumi, MD, PhD; Yuji Soejima, MD, PhD; Tetsuo Ikeda, MD, PhD; and Yoshihiko Maehara, MD, PhD

Department of Surgery and Science, Graduate School of Medical Sciences, Kyushu University, Fukuoka 812-8582, Japan

Key words: autophagy, cancer progression, hepatocellular carcinoma

Word count: Summary, 215 words; Text, 3970 words

Tables (2) and Figures (4)

Supporting information: 3 tables, 3 figures, Materials and Methods details (1327 words)

Corresponding author: Ken Shirabe, MD, PhD

Department of Surgery and Science, Graduate School of Medical Sciences, Kyushu

University, 3-1-1 Maidashi, Higashi-ku, Fukuoka 812-8582, Japan.

Tel: +81-92-642-5466. Fax: +81-92-642-5482. E-mail: kshirabe@surg2.med.kyushu-u.ac.jp

Abstract

Background: Several types of cancers, including hepatocellular carcinoma (HCC), show resistance to hypoxia and nutrient starvation. Autophagy is a means of providing macromolecules for energy generation under such stressed-conditions. The aim of this study was to clarify the role of autophagy in HCC development under hypoxic conditions.

Methods: The expression of microtubule-associated protein 1 light chain 3 (LC3), which is a key gene involved in autophagosome formation, was evaluated in human HCC using immunohistochemistry and western blot. The relationship between LC3 and hypoxia-induced factor 1 α (HIF1 α) expression was examined using real-time PCR. In addition, human HCC cell line Huh7 was treated with pharmacological autophagy-inhibitor and inactive mutant of Atg4B (Atg4B^{C74A}) under hypoxic condition to evaluate the effects of hypoxia-induced autophagy on cell survival, intracellular ATP, and mitochondrial β -oxidation.

Results: LC3 was significantly highly expressed in HCC as compared with noncancerous tissues. LC3 expression, correlated with HIF1 α expression, was also significantly correlated with tumor size, and only in the context of large tumors, was an independent predictor of HCC recurrence after surgery. In addition, Huh7 treated with autophagy-inhibitor under hypoxia had lower viability, with low levels of intracellular ATP due to impaired mitochondrial β -oxidation.

Conclusions: Autophagy in HCC works to promote HIF1 α -mediated proliferation through the maintenance of intracellular ATP, depending on the activation of mitochondrial β -oxidation. These findings demonstrated the feasibility of anti-autophagic treatment as a potential curative therapy for HCC, and improved understanding of the factors determining adaptive metabolic responses to hypoxic conditions.

Abbreviations:

AFP, alpha-fetoprotein

Atg, autophagy-related genes

ATP, adenosine 5'-triphosphate

DCP, des-gamma-carboxy prothrombin

HCC, hepatocellular carcinoma

HIF1 α , hypoxia-induced factor 1 α

ICG R15, indocyanine green retention test at 15 min

LC3, microtubule-associated protein 1 light chain 3

PBS, phosphate-buffered saline

PCR, polymerase chain reaction

PI3K, phosphatidylinositol 3-kinase

ROS, reactive oxygen species

SD, standard deviation

3MA, 3-methyladenine

INTRODUCTION

Hepatocellular carcinoma (HCC) is common and increasing in incidence worldwide.^{1,2} HCC grows to a relatively large size, sometimes over 10 cm in diameter even when necrosis was observed⁵ and it can easily reoccur after therapy.⁶ Proliferating cancer cells in tumors growing to a large size require a good supply of nutrients and oxygen. Angiogenesis around tumors is one way of increasing blood flow to provide the required oxygen and energy to the growing tumor.⁷ However, recent studies have revealed that nutrition levels, oxygen and glucose are frequently reduced in locally advanced tumors despite tumor vessels having been established.^{8,9} This suggests that the microvasculature around the tumor is structurally and functionally abnormal and not capable of supplying the blood flow needed for cancer cell growth. Furthermore, some aggressive malignant tumors, such as poorly differentiated HCC and pancreatic cancers, are clinically hypovascular.¹⁰ Under these conditions, cancer cells are likely to encounter limited nutrients and oxygen. However, they can exhibit resistance to nutrient deprivation and continue to grow. The mechanisms by which cancer cells obtain energy sources when their external nutrient supply is limited remain unclear.

Autophagy is a homeostatic mechanism that regulates the turnover of long-lived or damaged proteins and organelles, buffers intracellular constituents and supplies amino acids taken from degradation products of the autolysosome.¹¹ For the first step, the isolation membrane, a lipid bilayer structure, is developed and sequesters cytoplasmic materials such as organelles, to form autophagosomes. During this step, microtubule-associated protein 1 light chain 3 (LC3), one of the mammalian homologues of yeast autophagy-related gene (Atg) 8, is processed and activated by a ubiquitination-like reaction regulated by Atg7 and Atg3.¹² First, LC3 proform is cleaved into a soluble form known as LC3-I, which is further modified into a membrane-bound form, LC3-II, and this is followed by recruitment into the autophagosomes. Thus, LC3 is a specific marker of autophagosome formation. Autophagosomes engulf organelles and then fuse with lysosomes to become mature autolysosomes. Accordingly,

sequestered materials are digested into amino acids in the autolysosomes by the lysosomal enzymes.^{13, 14}

To study the role of autophagy in HCC under hypoxia-induced metabolic stress, we examined LC3 expression as the main marker of autophagosomes, and the other corresponding autophagic genes, Atg5 and Beclin-1, in human tissue samples and HCC cell lines under hypoxic conditions. Our results suggest that high expression of autophagy has the potential to cause malignant tumors to grow in size under hypoxic condition and also promotes poor survival, which can be independently predicted by the autophagic gene LC3 in HCC.

MATERIALS AND METHODS

Human Tissue Samples

Samples from 102 patients who had undergone liver resection for HCC without preoperative treatment at the Department of Surgery and Science at the Kyushu University Hospital between January 1986 and December 2002 were analyzed using immunohistochemistry.¹⁵ Samples from another 131 patients between January 2004 and March 2009 were analyzed by real-time polymerase chain reaction (PCR). There were no significant differences between the characteristics of HCC patients using immunohistochemistry analysis or real-time PCR analysis (Table S1). Details in Doc. S1.

Reagents and Plasmid

3-Methyladenine (3MA) and an inactive mutant of Atg4B (Atg4B^{C74A}) were prepared as described previously.^{15,16} Details in Doc. S1.

Immunohistochemistry and Immunofluorescence

Immunohistochemical staining and immunofluorescence analysis was performed as previously described.¹⁷⁻²⁰ Immunoreactivity of cytoplasmic staining in the cancerous region was independently divided into two groups, positive and negative, by two liver pathologists. Positive staining was classified if even a small area of tissue was stained. Details in Doc. S1.

Protein Extraction and Western Blot Analysis

Protein extraction and western blot analysis were performed as previously described.²¹ Details in Doc. S1.

Real-Time PCR

Extraction of total RNA and real-time PCR was performed as previously described.²²

Primers used for real-time PCR are shown in Table S2 and details described in Doc. S1.

Electron Microscopy

Analysis of electron microscopy was performed as previously described.^{20, 23, 24} For quantification of autophagosome using electron micrographs, high-powered micrographs (x8000-10000) of 10 single cells from multiple distinct low-powered fields were obtained from each specimen.²³ Details in Doc. S1.

Cell Culture under Hypoxic Conditions

For hypoxia treatments, human HCC cell lines were incubated in a humidified hypoxic workstation (MCO-5M, Sanyo, Osaka, Japan) with final oxygen concentrations of 0.1% O₂ using a Clark-type polarographic electrode (Animas, Frazer, PA, USA). To defect autophagosome formation, cultured cells were treated with autophagy-inhibitor using two methods, 3MA and Atg4B^{C74A}, and pre-incubated for 24 hours followed by incubation under hypoxia. Details in Doc. S1.

Quantification of Intracellular ATP

Total cellular ATP concentration was quantitated using an ATP Detection Reagent kit (Toyo-ink, Tokyo, Japan) as previously described.²⁵ Details in Doc. S1.

Cytofluorimetric Analysis of $\Delta\Psi_m$ and Mitochondrial Structure

Cytofluorimetric analysis of $\Delta\Psi_m$ and alteration of mitochondrial structure during hypoxia was performed as previously described.^{26, 27} Details in Doc. S1.

Measurement of β -hydroxybutyrate

β -hydroxybutyrate concentration was spectrophotometrically assayed as previously

described.²⁸ Details in Doc. S1.

Statistical Analysis

All statistical analyses were performed using JMP statistical software version 7.01 (SAS Institute Inc., Cary, NC, USA). All experiments were independently performed three times in triplicate. All variables are expressed as the mean \pm standard deviation (SD). Details in Doc. S1.

RESULTS

Upregulation of LC3 expression and Autophagy Activation in HCC

In the cancer cells of 102 HCC resected tissues, LC3 immunoreactivity was observed in the cytoplasm in 49 of 102 specimens (Fig. 1A). LC3 immunoreactivity was not observed in noncancerous lesions in any specimens. Western blot analysis using a limited set of tissue samples consisting of four matched noncancerous and HCC tissues revealed that expression of LC3-II, a well-known marker of activated autophagy, was detected in the cancerous tissue of case 3 and 4, in which LC3 immunoreactivity was immunohistochemically observed in the cancer cells (Fig. 1B). p62 regulates ubiquitin-positive protein aggregates caused by autophagic deficiency. Considering the results that the expression of p62 were higher in Case 1 and 2 than in Case 3 and 4 both at the cancerous and noncancerous tissues, it also indicated that the autophagic activity were impaired even in the noncancerous tissue and highly impaired in cancerous lesions in the Case 1 and 2.

Relationship between LC3 Expression and Clinicopathological Factors

The positive LC3 expression group had significantly higher serum tumor markers, AFP (P = 0.0467) and DCP (P = 0.0454), tumor size (P = 0.0006) and positive rates of portal vein invasion (P = 0.0001) than the negative LC3 expression group (Table 1). Unexpectedly, there were no correlation between the LC3 expression and viral infection. Some patients with HCV or HBV underwent the each pharmacological therapy such as interferon or nucleotide analog, therefore, the activities of hepatitis were difficult to be assessed accurately. That might be the reason why the autophagic activity was necessarily correlated with the presence of the hepatitis clinically.

Association of LC3 with HIF1 α Expression and HCC recurrence according to HCC Tumor Size

LC3 (Fig. 1C, $P = 0.0131$) and HIF1 α (Fig. 1D, $P = 0.0089$) expression was correlated with tumor size. In the group with a tumor size of ≥ 3 cm (Fig. 1E), LC3 expression in the high HIF1 α expression group was greater than in the low HIF1 α expression group ($P = 0.0097$). In any case, LC3 expression in the positive recurrence group was higher than in the negative recurrence group (Fig. 1F, $P = 0.0088$), whereas, in the group with a tumor size of < 3 cm, there was no difference in LC3 expression between the high and low HIF1 α expression groups (Fig. 1G and 1H). These indicated that only in the case of larger tumors, in which hypoxia and poor nutritional conditions were indicated, the autophagic gene LC3 was highly expressed and that autophagy enhanced tumor growth and promoted HCC malignancy.

Association of High Expression of LC3 with Tumor Size and Poor HCC Prognosis

For the entire patient group ($n = 131$), the disease-free survival rates of the positive LC3 group (49.0 % at 3 years and 34.7 % at 5 years) was lower than for the negative LC3 group (60.4 % at 3 years and 46.8 % at 5 years) ($P = 0.0056$) (Fig. 2A). In patients with a tumor size of ≥ 3 cm ($n = 65$), disease-free survival in the positive LC3 group (48.4 % at 3 years and 32.3 % at 5 years) was lower than in the negative LC3 group (82.6 % at 3 years and 59.8 % at 5 years) ($P = 0.0054$) (Fig. 2B). In contrast, in patients with a tumor size of < 3 cm ($n = 66$), there was no difference (Fig. 2C).

Prognostic Value of LC3 Expression in HCC Patients with a Tumor Size of ≥ 3 cm

The prognostic factors were evaluated in patients with a tumor size of ≥ 3 cm using univariate analysis (Table S3), which showed that three parameters namely, ICG R15 ($P = 0.0001$), multiple tumors ($P = 0.0416$) and portal vein invasion ($P = 0.0280$) were predictors of HCC recurrence. Positive LC3 expression was also a predictor of tumor recurrence ($P = 0.0103$). Furthermore, multivariate analysis was conducted with four of the variables (positive LC3 expression, ICG R15 $\geq 14.5\%$ as median values, multiple tumors and portal vein

invasion), and there was no obvious correlation between them (Table 2). Positive LC3 expression was still the independent variable for predicting poor disease free survival ($P = 0.0065$).

Upregulation of LC3 expression in HCC Cell Lines under Hypoxic Conditions

Hypoxia markedly increased the number of autophagic vacuoles in Huh7 cells, which appeared as dot-like signals by immunofluorescence analysis (Fig. 3A, 3B) and electron microscopy (Fig. 3C, 3D). Expression of LC3-II increased in a time dependent manner (Fig. 3E). These initial observations indicated that HCC cell lines had the potential power to express autophagic activity in response to hypoxic conditions.

Suppression of Autophagy and Proliferation of HCC Cells under Hypoxic Conditions

LC3 expression was suppressed using two methods namely, pharmacological inhibition by means of 3MA and transfection of Atg4B^{C74A}, which involved type III PI3K inhibition and hampering of the conversion of LC3-I to LC3-II, respectively (Fig. S1). Subsequently, the down-regulation of autophagy under hypoxia inhibited the proliferation of HCC cells (Fig. 4A). In addition, the growth of Huh7 cells transfected with GFP-LC3 was higher than the cells receiving no treatment under hypoxic condition (Fig. 4A). These findings indicated that hypoxia-induced autophagy in HCC cells works to promote cell proliferation through preventing accumulation of damaged protein and organelles.

Suppression of Autophagy Activity and Mitochondrial β -Oxidation

The levels of intracellular ATP in autophagy-inhibited HCC cells were lower than in non-treated cells (Fig. 4B). The proportion of HCC cells with low mitochondria membrane permeability treated with autophagy-inhibitor was higher (Fig. 4C). Gene expression levels of MCAD and CPT, L-FABP, and FATP enzymes in autophagy-inhibited cells, which were

indicated to have a rate-controlling effect on β -oxidation, the transportation of free fatty acids to mitochondria, and the transport of free fatty acids into hepatocytes, respectively, were significantly lower than those in non-treated cells (Fig. 4D). Consequently, β -hydroxybutyrate levels, final ketone body product, in autophagy-inhibited cells were decreased more than in non-treated cells (Fig.4E). These findings indicated that HCC cells exposed to hypoxia had the potential power to maintain intracellular ATP through the activation of mitochondrial β -oxidation, which may have been due to the prompt removal of the damaged mitochondria by activated autophagy as a selective degradation system.

DISCUSSION

In the present study, the inalterable role of autophagy in human HCC exposed to hypoxic conditions as tumors grew in size was demonstrated. The LC3 expression was correlated with tumor size, and only in large tumors, was correlated with the expression of HIF1 α , hypoxia and the under nutrition marker. Additionally, high expression of LC3 was shown to be an independent predictor of HCC recurrence. Further, analysis of HCC cell lines using autophagy-inhibitor revealed that the hypoxia-induced autophagy in HCC cells worked to promote cell proliferation through maintenance of intracellular ATP. This depended on the activation of mitochondrial β -oxidation with the prompt removal of damaged mitochondria due to activated autophagy. This is the first report demonstrating the mechanism involved in maintaining the intracellular energy sources by means of activated autophagy, as HCC tumors developed in large size under hypoxic stress. Recently some reports demonstrated that the emerging role of autophagy for promoting cell viability in HCC progressions during ischemia-hypoxia condition only in the rodent models.^{29, 30} We also demonstrated these results even in human samples clinically and emphasized that ‘only in the large tumors’ in which the impact of hypoxia and poor conditions were involved, the autophagic activity was highly expressed and its enhancement for the tumor growth and promotion of HCC malignancy, therefore, the newly targeted therapy for autophagy pathway of these adaptive metabolic responses is desired to become major challenges to overcome the large sized HCC tumors.

The role of autophagy in cell fate decision remains controversial. Autophagy is claimed to be an indispensable physiological reaction that sustains cell viability under nutrient-starved conditions.³¹ Regarding cancer cells, it has been reported that autophagy was highly expressed in many of these cells and that this high expression was a strong factor related to tumor progression.³² However, autophagy has recently attracted attention in connection with programmed or autophagic cell death. Colell et al.³³ demonstrated that cell death resulting from progressive cellular consumption can be attributed to unrestrained autophagy, which has

led to the belief that autophagy is a nonapoptotic form of programmed cell death.^{34,35} However, the role of autophagy, an alternative caspase-independent cell death program, and its underlying molecular mechanism, is still controversial in cancer, especially in tumor progression. About the mTOR pathway, mTOR inhibitors such as RAD001, also an autophagy inducer, does not promote the proliferation of HCC cells and results in cell death.^{36,37} Weiner LM, et al.³⁸ demonstrated that autophagy is observed in established cancers, but its inhibition during early carcinogenesis actually promotes tumor progression, suggesting that an autophagic switch promotes the transition of a tumor into a state of so-called autophagy addiction in order to maintain viability in hypoxic, nutrient-limited microenvironments. They also discussed that the autophagic function depends on the extent to which cells are capable of enhancing basal levels of autophagy. In fact, the hyperdynamic state of autophagy might be the crisis of cellular life because of its consumption of the intracellular even healthy organelle and proteins. Considering the reports of mTOR inhibitors resulted in HCC cell death, the basal levels of autophagy in these setting of HCC cells and whether its inhibitor might excessively induce the autophagic activity or not should be carefully assessed because mTOR is a strong key component in a series of pathways involved in tumor growth and development. We revealed the protective role played by autophagy that involves proliferation of HCC cells due to activation of mitochondrial β -oxidation. Furthermore, we investigated the clinical significance of this finding regarding the link between autophagy and tumor progression. Three HIF1 α -dependent molecular mechanisms have been reported by which cells adapt their energy metabolism under hypoxic conditions: inhibition of mitochondrial biogenesis by repression of c-Myc activity;³⁹ inhibition of acetyl-CoA synthesis by activation of PDK1;⁴⁰ and COX4 subunit switching.⁴¹ We demonstrated that protection of mitochondria by autophagy is a fourth component of the HIF1 α -mediated metabolic adaptation required to prevent cell death and damaged mitochondria, due to increased ROS levels in HCC cells under low nutrient conditions.

Ding et al.⁴² demonstrated that only in an apoptosis compromised background, the expression of the autophagic gene, Beclin 1, and their corresponding autophagic activities were suppressed in HCC. They indicated that the loss of a survival pathway, autophagy, enhanced tumor growth by promoting genome damage and instability in an apoptosis-deficient background, a Bcl-xL positive background. However, their data depended on the assessment of the expression of Beclin-1 and there were multiple molecular machineries involved in the formation of the autophagosome downstream of Beclin-1. Therefore, it was not established whether autophagy was truly activated.³⁹ Recently, some reports demonstrated Beclin-1 independent autophagy, which acted as a caspase-independent cell death mechanism.⁴³⁻⁴⁵ Additionally, Beclin-1 is the multifunctional gene involved in apoptosis.^{46, 47} Thus, Beclin-1 plays a key role in autophagy, however, Beclin-1 should be carefully analyzed for the assessment of activated autophagy. The standard method for assessing autophagic activity is the demonstration of autophagic vesicles using electron microscopy,⁴⁸ and another method is the LC3-based assay. When autophagy occurs, conversion of a fraction of the cytosolic form of LC3-I to the autophagic membrane form of LC3-II can be detected using western blots of LC3 proteins. This change in intracellular localization of LC3 protein is considered to correlate with autophagic activity,⁴⁹ and LC3 expression detected using immunohistochemistry represents the steady-state LC3 level including both LC3-I and LC3-II. We examined activated autophagy promptly with LC3-II using western blotting and confirmed the high expression of autophagosomes using an electron microscope.

Regarding the energy supply system in surviving cancer cells, several cancer cell lines including pancreatic cancer-derived and colorectal cancer-derived cell lines, are resistant to nutrient-deprived culture conditions.⁵⁰ These cells might use some alternative metabolic process to obtain energy for survival. However, untransformed human fibroblasts were completely abolished under the same conditions.⁵¹ These indicated that this phenomenon of

starvation-resistance may contribute to survival of cancer cells in nutrient-deficient microenvironments. As an alternative energy source, mammalian cells can use amino acids.⁵² If the starvation-resistant cancer cells can raise amino acids from the inside of cells, these amino acids become potential energy sources. Autophagy is an evolutionarily conserved process involving lysosomal degradation of cytoplasmic and cellular organelles.^{11,26} Autophagy constitutes a stress adaptation that avoids tumor death and has roles in protecting cells against the shortage of nutrients.^{26,53} Furthermore, autophagy is a catabolic process by which cells supply amino acids from self-digested organelles, as an alternative energy source for survival.^{11,13,31} This function of autophagy seems ideal in fostering the survival of cancer cells in an unfavorable starved microenvironment. We demonstrated that autophagy plays an essential role by maintaining an optimal balance between the competing demands of energy and proliferation under hypoxic conditions. Whereas consideration of cellular energetics favors oxidative metabolism as the most efficient means of producing adequate levels of ATP to maintain cell survival, mitochondrial respiration is also associated with increased amino acid consumption due to autophagy. It was reasonable that the two aspects of HIF1 α mediated-autophagic function, namely the protection of mitochondria and the supply amino acids from inside the cell contributed to cell survival in response to hypoxia.

For the recurrence of HCC after surgery, high expression of LC3 is the independent predictive factor in the context of larger sized tumors. Other predictive factors were liver dysfunction defined as ICG R15 < 14.5%, multiple tumors and portal vein invasion. As HCC tumors grow, it becomes difficult to secure an exogenous energy supply, in particular for the central nest of tumors. However, in small HCC tumors with adequate oxygen supply and enriched nutrient conditions, cells did not struggle to obtain energy from an exogenous nutrient supply. For this reason, in patients with tumors of < 3 cm, there was no correlation between LC3 expression, and HIF1 α expression and tumor size. However, in patients with tumors of \geq 3 cm, LC3 expression was significantly associated with HIF1 α expression. To

curatively treat HCC, an effective approach may be not only to inhibit the autophagy machinery, but also the HIF1 α machinery molecule to prevent energy supply in conditions in which exogenous nutrient supply is extremely limited.

We have provided experimental evidence supporting the conclusion that HIF1 α -mediated autophagy is involved in mitochondrial metabolism and is essential to understanding the mechanisms and consequences of the maintenance of intracellular energy in cancer cells under hypoxic conditions. This process requires the HIF1 α -dependent induction of autophagy machinery as demonstrated by means of LC3-deficient HCC cell analysis. Understanding the factors determining which of these adaptive metabolic responses to conditions of hypoxia and under nutrition in HCC cells are utilized *in vitro* and *in vivo*, and whether these adaptations are successful in preventing cell death, remains a challenge.

ACKNOWLEDGMENTS

We are grateful to T. Yoshimori (Osaka University) for kindly providing the inactive mutant of Atg4B (Atg4B^{C74A}). We also thank N. Yamashita (Kyushu University) for her expert advice related to statistical analysis.

DISCLOSURE STATEMENT

The authors have no conflicts of interest to declare and have no financial interests linked to this work.

REFERENCES

1. Shirabe K, Toshima T, Taketomi A, et al. Hepatic aflatoxin B1-DNA adducts and TP53 mutations in patients with hepatocellular carcinoma despite low exposure to aflatoxin B1 in southern Japan. *Liver Int.* 2011; 31:1366-72.
2. Shirabe K, Itoh S, Yoshizumi T, et al. The predictors of microvascular invasion in candidates for liver transplantation with hepatocellular carcinoma-with special reference to the serum levels of des-gamma-carboxy prothrombin. *J Surg Oncol.* 2007; 95:235-40.
3. Shirabe K, Kajiyama K, Harimoto N, Tsujita E, Wakiyama S, Maehara Y. Risk factors for massive bleeding during major hepatectomy. *World J Surg.* 2010; 34:1555-62.
4. Bruix J, Llovet JM. Prognostic prediction and treatment strategy in hepatocellular carcinoma. *Hepatology* 2002; 35:519-24.
5. Yamashita Y, Taketomi A, Shirabe K, et al. Outcomes of hepatic resection for huge hepatocellular carcinoma (≥ 10 cm in diameter). *J Surg Oncol.* 2011; 104:292-8.
6. Taketomi A, Sanefuji K, Soejima Y, et al. Impact of des-gamma-carboxy prothrombin and tumor size on the recurrence of hepatocellular carcinoma after living donor liver transplantation. *Transplantation.* 2009; 87:531-7.
7. Vaupel P, Thews O, Hoehckel M. Treatment resistance of solid tumors: role of hypoxia and anemia. *Med Oncol.* 2001; 18:243-59.
8. Jain RK. Molecular regulation of vessel maturation. *Nat Med.* 2003; 9:685-93.
9. Harris AL. Hypoxia – a key regulatory factor in tumour growth. *Nat Rev Cancer.* 2002; 2:38-47.
10. Kitano M, Kudo M, Maekawa K, et al. Dynamic imaging of pancreatic diseases by contrast enhanced coded phase inversion harmonic ultrasonography. *Gut* 2004; 53:854-9.
11. Klionsky DJ, Emr SD. Autophagy as a regulated pathway of cellular degradation. *Science* 2000; 290:1717–21.
12. Tanida I, Tanida-Miyake E, Ueno T, Kominami E. The human homolog of

- Saccharomyces cerevisiae* Apg7p is protein-activating enzyme for multiple substrates including human Apg12p, GATE-16, GABARAP, and MAP-LC3. *J Biol Chem.* 2001; 276:1701-6.
13. Mizushima N, Yoshimori T, Levine B. Methods in mammalian autophagy research. *Cell* 2010; 140:313-26.
 14. Fleming A, Noda T, Yoshimori T, Rubinsztein DC. Chemical modulators of autophagy as biological probes and potential therapeutics. *Nat Chem Biol.* 2011; 7:9-17.
 15. Liver Cancer Study Group. The general rules for the clinical and pathological study of primary liver cancer, 7th edn. Tokyo: Kanehara Publications; 2006.
 16. Fujita N, Hayashi-Nishino M, Fukumoto H, et al. An Atg4B mutant hampers the lipidation of LC3 paralogues and causes defects in autophagosome closure. *Mol Biol Cell.* 2008; 19:4651-9.
 17. Aishima S, Fujita N, Mano Y, et al. Different roles of S100P overexpression in intrahepatic cholangiocarcinoma: carcinogenesis of perihilar type and aggressive behavior of peripheral type. *Am J Surg Pathol.* 2011; 35:590-8.
 18. Kabeya Y, Mizushima N, Yamamoto A, Oshitani-Okamoto S, Ohsumi Y, Yoshimori T. LC3, GABARAP and GATE16 localize to autophagosomal membrane depending on form-II formation. *J Cell Sci.* 2004; 117:2805-12.
 19. Mizushima N, Yoshimori T, Levine B. Methods in mammalian autophagy research. *Cell.* 2010;140:313-26.
 20. Klionsky DJ, Abdalla FC, Abeliovich H, Abraham RT, Acevedo-Arozena A, Adeli K, et al. Guidelines for the use and interpretation of assays for monitoring autophagy. *Autophagy.* 2012;8:445-544.
 21. Anegawa G, Kawanaka H, Yoshida D, et al. Defective endothelial nitric oxide synthase signaling is mediated by rho-kinase activation in rats with secondary biliary cirrhosis. *Hepatology* 2008; 47:966-977.

22. Sadagurski M, Cheng Z, Rozzo A, et al. IRS2 increases mitochondrial dysfunction and oxidative stress in a mouse model of Huntington disease. *J Clin Invest.* 2011; 121:4070-81.
23. Nanjundan M, Nakayama Y, Cheng KW, et al. Amplification of MDS1/EVI1 and EVI1, located in the 3q26.2 amplicon, is associated with favorable patient prognosis in ovarian cancer. *Cancer Res.* 2007; 67:3074-84.
24. Klionsky DJ, Abeliovich H, Agostinis P, Agrawal DK, Aliev G, Askew DS, et al. Guidelines for the use and interpretation of assays for monitoring autophagy in higher eukaryotes. *Autophagy.* 2008;4:151-75.
25. Kasahara A, Ishikawa K, Yamaoka M, et al. Generation of trans-mitochondrial mice carrying homoplasmic mtDNAs with a missense mutation in a structural gene using ES cells. *Hum Mol Genet.* 2006; 15:871-81.
26. Du H, Yang W, Chen L, Shen B, Peng C, Li H, et al. Emerging role of autophagy during ischemia-hypoxia and reperfusion in hepatocellular carcinoma. *Int J Oncol.* 2012;40:2049-57.
27. Chang Y, Yan W, He X, Zhang L, Li C, Huang H, et al. miR-375 inhibits autophagy and reduces viability of hepatocellular carcinoma cells under hypoxic conditions. *Gastroenterology.* 2012;143:177-87.
28. Petit PX et al. Alterations in mitochondrial structure and function are early events of dexamethasone-induced thymocyte apoptosis. *J Cell Biol.* 1995; 130:157-67.
29. Hanson GT, Aggeler R, Oglesbee D, et al. Investigating mitochondrial redox potential with redox-sensitive green fluorescent protein indicators. *J Biol Chem.* 2004; 279:13044-53.
30. Aleksunes LM, Reisman SA, Yeager RL, Goedken MJ, Klaassen CD. Nuclear factor erythroid 2-related factor 2 deletion impairs glucose tolerance and exacerbates hyperglycemia in type 1 diabetic mice. *J Pharmacol Exp Ther.* 2010; 333: 140-51.

31. Levine B, Klionsky DJ. Development by self-digestion: molecular mechanisms and biological functions of autophagy. *Dev Cell*. 2004; 6:463–77.
32. Kuwahara Y, Oikawa T, Ochiai Y, et al. Enhancement of autophagy is a potential modality for tumors refractory to radiotherapy. *Cell Death Dis*. 2011; 2:e177.
33. Colell A, Ricci JE, Tait S, et al. GAPDH and autophagy preserve survival after apoptotic cytochrome c release in the absence of caspase activation. *Cell* 2007; 129:983-7.
34. Kirkegaard K, Taylor MP, Jackson WT. Cellular autophagy: surrender, avoidance and subversion by microorganisms. *Nat Rev Microbiol*. 2004; 2:301–14.
35. Kondo Y, Kanzawa T, Sawaya R, Kondo S. The role of autophagy in cancer development and response to therapy. *Nat Rev Cancer*. 2005; 5:726–34.
36. Thomas HE, Mercer CA, Carnevalli LS, Park J, Andersen JB, Conner EA, et al. mTOR inhibitors synergize on regression, reversal of gene expression, and autophagy in hepatocellular carcinoma. *Sci Transl Med*. 2012;4:139ra84.
37. Altmeyer A, Josset E, Denis JM, Gueulette J, Slabbert J, Mutter D, Noël G, Bischoff P. The mTOR inhibitor RAD001 augments radiation-induced growth inhibition in a hepatocellular carcinoma cell line by increasing autophagy. *Int J Oncol*. 2012 Aug 7.
38. Weiner LM, Lotze MT. Tumor-cell death, autophagy, and immunity. *N Engl J Med*. 2012;366:1156-8.
39. Lu Z, Dono K, Gotoh K, et al: Participation of autophagy in the degeneration process of rat hepatocytes after transplantation following prolonged cold preservation. *Arch Histol Cytol*. 2005; 68:71-80.
40. Degenhardt K, Mathew R, Beaudoin B, et al: Autophagy promotes tumor cell survival and restricts necrosis, inflammation, and tumorigenesis. *Cancer Cell*. 2006; 10:51-64.
41. Pouyssegur J, Dayan F, and Mazure NM. Hypoxia signalling in cancer and approaches to enforce tumour regression. *Nature* 2006; 441:437-443.
42. Ding ZB, Shi YH, Zhou J, et al. Association of autophagy defect with a malignant

- phenotype and poor prognosis of hepatocellular carcinoma. *Cancer Res.* 2008; 68:9167-75.
43. Scarlatti F, Maffei R, Beau I, Codogno P, Ghidoni R. Role of non-canonical Beclin 1-independent autophagy in cell death induced by resveratrol in human breast cancer cells. *Cell Death Differ.* 2008; 15:1318-29.
 44. Chu CT, Zhu J, Dagda R. Beclin 1-independent pathway of damage-induced mitophagy and autophagic stress: implications for neurodegeneration and cell death. *Autophagy* 2007; 3:663-6.
 45. Pickford F, Masliah E, Britschgi M, et al. The autophagy-related protein beclin 1 shows reduced expression in early Alzheimer disease and regulates amyloid beta accumulation in mice. *J Clin Invest.* 2008; 118:2190-9.
 46. Boya P, González-Polo RA, Casares N, et al. Inhibition of macroautophagy triggers apoptosis. *Mol Cell Biol.* 2005; 25:1025-40.
 47. Ait-Mohamed O, Battisti V, Joliot V, et al. Acetonic extract of *Buxus sempervirens* induces cell cycle arrest, apoptosis and autophagy in breast cancer cells. *PLoS One.* 2011; 6:e24537.
 48. Mizushima N, et al. Methods for monitoring autophagy. *Int J Biochem Cell Biol.* 2004;36:2491-2502.
 49. Kabeya Y, Mizushima N, Ueno T, et al. LC3, a mammalian homologue of yeast Apg8p, is localized in autophagosomal membranes after processing. *EMBO J.* 2000; 19:5720-8.
 50. Sato K, Tsuchihara K, Fujii S, et al. Autophagy is activated in colorectal cancer cells and contributes to the tolerance to nutrient deprivation. *Cancer res.* 2007; 67:9677-84.
 51. Esumi H, Izuishi K, Kato K, et al. Hypoxia and nitric oxide treatment confer tolerance to glucose starvation in a 5'-AMP-activated protein kinase-dependent manner. *J Biol Chem.* 2002; 277:32791-8.
 52. Kuma A, Hatano M, Matsui M, et al. The role of autophagy during the early neonatal

starvation period. *Nature* 2004; 432:1032-6.

53. Rouschop KM, van den Beucken T, Dubois L, et al. The unfolded protein response protects human tumor cells during hypoxia through regulation of the autophagy genes MAP1LC3B and ATG5. *J Clin Invest.* 2010; 120:127-41.

FIGURE LEGENDS

Figure 1. Upregulation of LC3 protein in HCC human tissue samples and HCC cell lines under hypoxic conditions.

(A) LC3 immunoreactivity was observed in the cytoplasm of cancer cells, and hepatocytes in non-cancerous tissues were negative for LC3. (B) Western blot analysis of LC3 expression in the four matched HCC tissues and noncancerous tissues. Expression of LC3-II was detected in cancerous tissue in case 3 and 4, but no or only a faint signal was detected in non-cancerous tissue all of the cases. The expression of p62 was higher in case 1 and 2 than in case 3 and 4. (C) (D) Huh7 cells exposed to 2 hours hypoxic conditions had markedly increased numbers of autophagic vacuoles, which appeared as dot-like signals by immunofluorescence analysis using antibody against LC3. (E) (F) Extensive autophagosome formation (arrowed) in Huh7 cells exposed to 2 hours hypoxic conditions was monitored using electron microscopy. (G) The expression of LC3-II increased in a time-dependent manner when evaluated by western blot analysis using the proteins extracted from Huh7 cells under hypoxic conditions for the indicated times. The expression of the other autophagic genes, Beclin-1 and Atg5, also increased in a time-dependent manner.

Atg, autophagy-related genes; HCC, hepatocellular carcinoma; LC3, microtubule-associated protein 1 light chain 3.

Figure 2. LC3 and HIF1 α expression associated with HCC tumor size. LC3 and HIF1 α expression were evaluated by real-time PCR analysis of human HCC samples. The analysis was performed on the three cohorts: (A) and (B), the total patient population (n = 131); (C), patients with tumor sizes of ≥ 3 cm (n = 65); and (D), patients with tumor sizes of < 3 cm (n = 66). They were also divided into two groups consisting of those with high and low expression of HIF1 α with a cutoff value with a median of 2.85.

LC3 (A) and HIF1 α (B) expression was significantly correlated with tumor size (LC3, $P = 0.0131$; HIF1 α , $P = 0.0089$). (C) In the group with a tumor size of ≥ 3 cm, LC3 expression in the high HIF1 α expression group was significantly greater than that in low HIF1 α expression group ($P = 0.0097$) and LC3 expression in the positive recurrence group was significantly higher than in the negative recurrence group ($P = 0.0088$). (D) In the group with a tumor size of < 3 cm, there was no significant difference in LC3 expression between the high and low HIF1 α expression groups, and between positive and negative recurrence groups.

HCC, hepatocellular carcinoma; HIF1 α , hypoxia-induced factor 1 α ; LC3, microtubule-associated protein 1 light chain 3.

Figure 3. Association between LC3 expression and patients' prognosis depending on tumor size of HCC. The disease-free survival after surgery were compared between the positive and negative LC3 expression groups by immunohistochemical analysis. The analysis was performed on three cohorts: (A), the total patient group ($n = 102$); (B), patients with tumor sizes of ≥ 3 cm ($n = 54$); and (C), patients with tumor sizes of < 3 cm ($n = 48$).

(A) For the entire patient group, the disease-free survival rates of the positive LC3 group (49.0 % at 3 years and 34.7 % at 5 years) was significantly lower than that of the negative LC3 group (60.4 % at 3 years and 46.8 % at 5 years) ($P = 0.0056$). (B) In the patients with a tumor size of ≥ 3 cm, disease-free survival in the positive LC3 group (48.4 % at 3 years and 32.3 % at 5 years) was significantly lower than in the negative LC3 group (82.6 % at 3 years and 59.8 % at 5 years) ($P = 0.0054$). (C) In patients with a tumor size of < 3 cm there was no significant difference between the two groups.

HCC, hepatocellular carcinoma; LC3, microtubule-associated protein 1 light chain 3.

Figure 4. Impaired proliferation of HCC cell lines treated with autophagy-inhibitor and deterioration of intracellular ATP maintenance through impairment of mitochondrial

β -oxidation due to suppressed autophagy activity. Huh7 cells receiving no treatment or treated with autophagy-inhibitor using two methods, pharmacological inhibitor as 3MA and transfection of Atg4B^{C74A}, were incubated under hypoxic conditions of 0.1% O₂ final concentration for 2 hours.

(A) Growth of both Huh7 cells treated using the two methods of autophagy-inhibition were significantly lower than that of the cells receiving no treatment under hypoxic conditions. (B) The intracellular ATP in the Huh7 cells treated with autophagy-inhibitor under hypoxic conditions was present at significantly lower levels than in cells receiving no treatment. (C) The proportion of Huh7 cells with low levels of mitochondrial membrane permeability treated with autophagy-inhibitor was higher than that of non-treated cells by FACS analysis using JC-1 antibody. (D) The gene expression related to mitochondrial β -oxidation in Huh7 cells were examined by real-time PCR. The levels of the enzymes MCAD and CPT, L-FABP, and FATP in Huh7 cells treated with autophagy-inhibitor were significantly lower than that in non-treated cells. (E) The intracellular β -hydroxybutyrate levels in Huh7 cells treated with autophagy-inhibitor under hypoxic conditions were significantly lower than in cells receiving no treatment.

ACC, acetyl-CoA carboxylase; ATP, adenosine 5'-triphosphate; CPT, carnitine palmitoyltransferase; FAS, fatty acid synthase; FAT, fatty acid translocase; FATP, fatty acid transport protein; L-FABP, fatty acid binding protein; LC3, microtubule-associated protein 1 light chain 3; MCAD, medium-chain acyl-CoA dehydrogenase; PCR, polymerase chain reaction; 3MA, 3-methyladenine.

LIST OF THE SUPPORTING INFORMATION

Supplementary Tables

Table S1. Characteristics of HCC patients with immunohistochemistry analysis and real-time PCR analysis.

Table S2. Real-time PCR Primer Sequences

Table S3. Univariate Analysis of Risk Factors related to Recurrence after Surgery in Patients with HCC Tumors of ≥ 3 cm in Size

Supplementary Figure legends

Figure S1. Association between LC3 expression and patients' prognosis depending on tumor size of HCC.

Figure S2. Inhibition of autophagy activity in Huh7 cells exposed to hypoxic conditions.

Figure S3. Deterioration of mitochondrial damage due to suppressed autophagy activity.

Supplementary documents S1: Materials and methods

TABLES

Table 1. Immunohistochemical Analysis of the Correlation between LC3 Expression and Clinicopathologic Characteristics in Patients

Variables	LC3 expression (n = 102)		P value
	Negative (n = 53)	Positive (n = 49)	
Age (years)	65 ± 9	62 ± 10	0.1703
Gender (male, %)	77.4	83.7	0.4206
HBs-Ag positive (%)	18.9	22.5	0.6551
HCV-Ab positive (%)	66.0	59.2	0.4744
Serum Albumin (g/dL)	4.0 ± 0.4	4.0 ± 0.4	0.3922
Serum T-Bil (mg/dL)	0.9 ± 0.3	0.9 ± 0.3	0.9179
PT (%)	84.1 ± 17.2	87.2 ± 15.5	0.3881
AST (units/L)	49.9 ± 31.0	50.8 ± 24.8	0.8695
ALT (units/L)	51.3 ± 33.7	57.8 ± 51.0	0.4514
ICG R15 (%)	17.0 ± 9.1	15.9 ± 8.7	0.5286
Platelet (10 ⁴ /μL)	14.6 ± 7.9	14.9 ± 6.3	0.8053
Child-Pugh A/B, C (%)	86.3/13.7	82.1/17.9	0.5857
Serum AFP (ng/mL)	215 ± 568	14908 ± 63219	0.0468
Serum DCP (mAU/L)	1884 ± 7253	6284 ± 17143	0.0454
Liver cirrhosis (%)	23.5	20.4	0.7062
Tumor size (cm)	3.0 ± 0.4	5.0 ± 0.4	0.0006
Multiple tumors (%)	28.3	38.8	0.2620
Stage I, II/ III, IV (%)	66.0/34.0	59.2/40.8	0.4744
Differentiation			
Well, moderate/ poor (%)	75.5/24.5	61.2/38.8	0.1207
Portal vein invasion (%)	26.4	69.4	0.0001
Intrahepatic metastasis (%)	13.2	33.3	0.1520

Data are expressed as the mean \pm standard deviation. AFP, alpha-fetoprotein; ALT, alanine aminotransferase; AST, aspartate aminotransferase; DCP, des-gamma-carboxyl prothrombin; HBs-Ag, hepatitis B surface antigen; HCC, hepatocellular carcinoma; HCV-Ab, hepatitis C virus antibody; ICG R15, indocyanine green retention rate at 15 min; LC3, microtubule-associated protein 1 light chain 3; PT, prothrombin time; T-Bil, total bilirubin.

Table 2. Multivariate Analysis of Risk Factors related to Postoperative Recurrence in Patients with HCC Tumors of ≥ 3 cm

Variables (n = 75)	Odds ratio	95% CI	P value
ICG R15 ≥ 14.5 (%)	6.306	2.471 - 22.704	0.0001
LC3	2.962	1.333 - 7.841	0.0065
Positive vs. negative			
Multiple tumors	2.626	1.152 - 7.210	0.0202
Positive vs. negative			
Portal vein invasion	2.200	1.012 - 5.439	0.0465
Positive vs. negative			

CI, confidence interval; HCC, hepatocellular carcinoma; ICG R15, indocyanine green retention rate at 15 min; LC3, microtubule-associated protein 1 light chain 3.

SUPPLEMENTARY TABLES

Table S1. Characteristics of HCC patients with immunohistochemistry analysis and real-time PCR analysis.

Variables	Patients with immunohisto-	Patients with real-time PCR	
Variables	chemistry analysis group	analysis group	P value
Variables	(n=102)	(n=131)	
Age (years)	63 ± 9	66 ± 11	0.0628
Gender (male, %)	80.4	75.6	0.3788
HBs-Ag positive (%)	20.6	11.7	0.0667
HCV-Ab positive (%)	62.7	68.7	0.3412
Serum Albumin (g/ dL)	4.0 ± 0.4	4.0 ± 0.4	0.7522
Serum T-Bil (mg/ dL)	0.9 ± 0.3	0.8 ± 0.4	0.5150
PT (%)	85.6 ± 16.4	86.1 ± 10.3	0.7576
AST (units/L)	50.3 ± 28.1	50.9 ± 34.0	0.8865
ALT (units/L)	54.4 ± 42.7	49.5 ± 35.6	0.3393
ICG R15 (%)	16.4 ± 8.9	15.1 ± 7.5	0.2154
Platelet (10 ⁴ / μL)	14.8 ± 7.1	15.3 ± 6.6	0.5759
Child-Pugh A/B, C (%)	84.4/ 15.6	85.9/ 14.1	0.3030
Serum AFP (ng/ mL)	7121 ± 43721	6332 ± 38181	0.0468
Serum DCP (mAU/ L)	3975 ± 13052	2610 ± 9135	0.3526
Liver cirrhosis (%)	23.7	25.4	0.2630
Tumor size (cm)	4.0 ± 2.9	3.7 ± 2.8	0.4755
Multiple tumors (%)	33.3	31.5	0.0743
Stage I, II/ III, IV (%)	62.7/ 37.3	67.7/ 32.3	0.4318
Differentiation			
well, moderate/poorly (%)	68.6/ 31.4	68.2/ 31.8	0.9469
Portal vein invasion (%)	47.1	35.9	0.0884
Intrahepatic metastasis (%)	22.8	25.6	0.2758

Mean \pm standard deviation. AFP, alpha-fetoprotein; ALT, alanine aminotransferase; AST, aspartate aminotransferase; DCP, des-gamma-carboxyl prothrombin; HBs-Ag, hepatitis B surface antigen; HCC, hepatocellular carcinoma; HCV-Ab, hepatitis C virus antibody; HIF1 α , hypoxia inducible factor 1 α ; ICG R15, indocyanine green retention rate at 15 minutes; LC3, microtubule-associated protein 1 light chain 3; PT, prothrombin time; T-Bil, total bilirubin.

Table S2. Real-time PCR Primer Sequences

Genes		Sequences
LC3	Sense	CCACACCCAAAGTCCTCACT
	Antisense	CACTGCTGCTTTCCGTAACA
β-actin	Sense	CAACTGGGACGACATGGAGAAAAT
	Antisense	CCAGAGGCGTACAGGGATAGCAC
Hif1α	Sense	GAAAGCGCAAGTCCTCAAAG
	Antisense	TGGGTAGGAGATGGAGATGC
MCAD	Sense	TGCTTTTGATAGAACCAGACCTACAGT
	Antisense	CTTGGTGCTCCACTAGCAGCTT
CPT	Sense	TCCATGCATACCAAAGTGGA
	Antisense	TGGT AGGAGAGAGCAGCACCTT
L-FABP	Sense	GCAGAGCCAGGAGAACTTTGAG
	Antisense	TTTGATTTTCTTCCCTTCATGCA
FAS	Sense	ATCCTGGAACGAGAACACGATCT
	Antisense	AGAGACGTGTCACTCCTGGACTT
ACC	Sense	GGGCACAGACCGTGGTAGTT
	Antisense	CAGGATCAGCTGGGATACTGAGT
FAT	Sense	CCAAATGAAGATGAGCATAGGACAT
	Antisense	GTTGACCTGCAGTCGTTTTGC
FATP	Sense	ACCACCGGGCTTCCTAAGG
	Antisense	CTGTAGGAATGGTGGCCAAAG

ACC, ace- tyl-CoA carboxylase; CPT, carnitine palmitoyltransferase; FAS, fatty acid synthase; FAT, fatty acid translocase; FATP, fatty acid transport protein; Hif1α, hypoxia-inducible factor 1α; LC3, microtubule-associated protein 1 light chain 3; L-FABP, fatty acid binding protein; MCAD, medium-chain acyl-CoA dehydrogenase.

Table S3. Univariate Analysis of Risk Factors related to Recurrence after Surgery in Patients with HCC Tumors of ≥ 3 cm in Size

Variables	Recurrence after surgery (n = 75)		P value
	Negative (n = 26)	Positive (n = 49)	
Age (years)	64 \pm 9	65 \pm 9	0.8375
Gender (male, %)	73.1	85.7	0.1894
HBs-Ag positive (%)	23.1	22.5	0.9508
HCV-Ab positive (%)	53.9	65.3	0.3340
Serum Albumin (g/dL)	4.0 \pm 0.3	3.9 \pm 0.3	0.0644
Serum T-Bil (mg/dL)	0.8 \pm 0.4	0.8 \pm 0.3	0.8170
PT (%)	90.4 \pm 15.1	85.9 \pm 15.1	0.2176
AST (units/L)	45.0 \pm 34.7	50.8 \pm 24.0	0.4016
ALT (units/L)	41.8 \pm 32.9	51.3 \pm 32.6	0.2321
ICG R15 (%)	9.2 \pm 6.9	18.9 \pm 7.6	0.0001
Platelet ($10^4/\mu\text{L}$)	9.1 \pm 10.6	5.9 \pm 7.9	0.1422
Child-Pugh A/B, C (%)	93.6/6.4	88.0/ 12.0	0.4220
Serum AFP (ng/mL)	2796 \pm 11840	14962 \pm 61979	0.3356
Serum DCP (mAU/L)	7184 \pm 16282	6366 \pm 17372	0.8455
Liver cirrhosis (%)	8.0	20.0	0.1668
Tumor size (cm)	6.1 \pm 3.6	5.3 \pm 2.8	0.3109
Multiple tumors (%)	34.6	59.2	0.0416
Stage I, II/ III, IV (%)	53.8/46.2	34.7/65.3	0.1099
Differentiation			
well, moderate/poor (%)	65.4/34.6	55.1/44.9	0.3870
Portal vein invasion (%)	30.8	57.1	0.0280
Intrahepatic metastasis (%)	23.1	43.8	0.0722

LC3 positive (%)	35.0	70.6	0.0103
------------------	------	------	--------

Data are expressed as the mean \pm standard deviation. AFP, alpha-fetoprotein; ALT, alanine aminotransferase; AST, aspartate aminotransferase; DCP, des-gamma-carboxyl prothrombin; HBs-Ag, hepatitis B surface antigen; HCC, hepatocellular carcinoma; HCV-Ab, hepatitis C virus antibody; ICG R15, indocyanine green retention rate at 15 min; LC3, microtubule-associated protein 1 light chain 3; PT, prothrombin time; T-Bil, total bilirubin.

SUPPLEMENTARY FIGURE LEGENDS

Figure S1. Inhibition of autophagy activity in Huh7 cells exposed to hypoxic conditions.

Huh7 cells receiving no treatment or treated with autophagy-inhibitor using two methods, pharmacological inhibitor as 3MA and transfection of Atg4B^{C74A}, were incubated under hypoxic conditions of 0.1% O₂ final concentration for 2 hours.

Atg, autophagy-related genes; LC3, microtubule-associated protein 1 light chain 3; 3MA, 3-methyladenine.

DOCUMENT S1: MATERIALS AND METHODS

Human Tissue Samples

Samples were collected immediately after resection, transported in liquid nitrogen and stored at -80°C. Histological diagnosis of the tumors was based on the General Rules for the Clinical and Pathological Study Group of Japan.¹⁵

The study protocol conformed to the ethical guidelines of the 1975 Helsinki Declaration and patient samples were collected after obtaining informed consent, according to an established protocol approved by the Ethics Committee of Kyushu University. The data do not contain any information that could lead to the identification of the patients.

Reagents and Plasmid

Antibodies were obtained from commercial sources as follows: rabbit polyclonal anti-LC3 antibody, rabbit polyclonal anti-Atg5 antibody and mouse monoclonal anti-p62 antibody from MBL (Nagoya, Japan); rabbit polyclonal anti-Beclin-1 antibody from Abcam (Cambridge, MA, USA); and mouse monoclonal anti- β -actin antibody from Santa Cruz Biotechnology (Santa Cruz, CA, USA). 3-Methyladenine (3MA), a widely used autophagy inhibitor of the type III PI3K¹⁴, was purchased from Sigma (St. Louis, MO, USA). An inactive mutant of Atg4B (Atg4B^{C74A}), a protease that processes pro-LC3 paralogs and hampers conversion of LC3-I to LC3-II, was kindly gifted from Dr. Yoshimori and prepared as described previously.¹⁶

Immunohistochemistry and Immunofluorescence

Paraffined 3- μ m sections of HCC samples were used for immunohistochemical staining that was performed as previously described.¹⁷ Briefly, the sections were deparaffinized, pretreated with autoclaving (121°C) for 15 min in 0.01mol/L citrate-buffered saline (pH 6.8) for antigen retrieval. Endogenous peroxidase activity was blocked by incubation with 0.3%

H₂O₂ for 10 min. The sections were incubated with antibody against LC3 at 4°C overnight. Streptavidin-biotin complex and horseradish peroxidase were applied, and the reaction products were visualized using the Histfine SAB-PO immunohistochemical staining kit (Nichirei, Tokyo, Japan), according to the manufacturers' instructions. Immunoreactivity of cytoplasmic staining in the cancerous region was independently divided into two groups, positive and negative, by two liver pathologists. Positive staining was classified if even a small area of tissue was stained.

Immunofluorescence analysis was performed as previously described.¹⁸ Cells plated in eight-chamber slides (Nunc, Rochester, NY, USA) were fixed with 4% paraformaldehyde, blocked using 0.1% albumin in phosphate-buffered saline (PBS) and then incubated with antibody against LC3 (dilution 1:500). Following washing with PBS, cells were incubated with Alexa488-labeled anti-rabbit IgG (Molecular Probes, Eugene, OR, USA) and visualized using a fluorescence laser scanning confocal microscope, BZ-8100 (Keyence, Tokyo, Japan). The total LC3 levels were realistically assessed by immunohistochemistry analysis because of the instability of LC3-II proteins in vivo samples by western blot analysis.^{19,20}

Protein Extraction and Western Blot Analysis

Protein extraction and western blot analysis were performed as previously described.¹⁹ Briefly, cells were lysed in a sodium dodecyl sulfate (SDS)-sample buffer containing 10% glycerol, 5% β-mercaptoethanol, 2.3% SDS and 62.5 mM Tris-HCl (pH 6.8). Protein (30 μg) was separated using SDS-PAGE and then transferred to polyvinylidene difluoride membranes. The membranes were washed, blocked and incubated with the specific primary antibody against Beclin-1 (dilution 1:1000), LC3 (dilution 1:1000), Atg5 (dilution 1:500), p62 (dilution 1:1000) and β-actin (dilution 1:2000), followed by incubation with horseradish peroxidase-conjugated secondary antibodies. The specific signals on the blot were visualized by enhanced chemiluminescence assay kit (ECL Plus Western Blotting Detection Reagents,

GE Healthcare, Buckinghamshire, UK).

Real-Time PCR

Total RNA was extracted from cell lines and frozen tumor specimens using the acid guanidinium thiocyanate/phenol/chloroform method. Following DNase treatment and reverse transcription (RT) using the SuperScript cDNA Synthesis Kit (Invitrogen, Carlsbad, CA, USA), real-time PCR was performed for 35 cycles of 15 s at 95°C and 60 s at 60°C using the StepOnePlus Real Time PCR System (Applied Biosystems, Foster City, CA) using a Quantitech SYBR Green PCR kit (Qiagen, Tokyo, Japan). Primers used for real-time PCR are shown in Supplementary Table 1. β -actin was used as an endogenous control to normalize for differences in the amount of total RNA in each sample. Relative expression of genes was calculated and expressed as $2^{-\Delta Ct}$, as described.²⁰

Electron Microscopy

Cells were immediately fixed with 2.5% glutaraldehyde with 0.1 mol/L PBS (pH 7.4) for 2 hours at 4°C. After washing with PBS, samples were postfixed with 2% osmium tetra oxide for 2 hours before being washed again in PBS, dehydrated in an ethanol and substitute propylene oxide to resin, then embedded in epoxy resin. After resin polymerization, sections (70nm) were cut with an ultramicrotome and double stained with uranyl acetate and lead solution. Electron micrographs were taken using HITACHI H-7500 transmission electron microscope. For quantification of autophagosome using electron micrographs, high-powered micrographs (x8000-10000) of 10 single cells from multiple distinct low-powered fields were obtained from each specimen.²¹ The maturation from the phagophore through the autophagolysosome is a dynamic and continuous process, and autophagosome or early autophagic vacuole (AVi) and degradative autophagic vacuole (AVd) were shown in electron microscopy.^{20, 24} The AVi could be identified by its contents such as morphologically intact cytoplasm, including ribosomes, and rough endoplasmic reticulum, and the AVd could be

detected by its limiting membrane partially visible as two bilayers separated by a narrow electron-lucent cleft as a double membrane. All of them were counted to the expression of autophagy.

Cell Culture under Hypoxic Conditions

Human HCC cell line, Huh-7, was routinely maintained in Dulbecco's modified Eagle's medium supplemented with 10% heat-inactivated fetal bovine serum, 100 units/mL penicillin and 100 mg/mL streptomycin sulfate (Life Technologies, Inc., Carlsbad, CA). For normoxia condition, cells were cultured at 37°C in a humidified incubator in an atmosphere of 5% CO₂. Meanwhile, for hypoxia treatments, cells were incubated in a humidified hypoxic workstation (MCO-5M, Sanyo, Osaka, Japan) with final oxygen concentrations of 0.1% O₂ using a Clark-type polarographic electrode (Animas, Frazer, PA, USA). To defect autophagosome formation, cultured cells were treated with autophagy-inhibitor using two methods. In the first, cells were incubated with 10mM of 3MA. In the second, cells were transiently transfected with Atg4B^{C74A} using Lipofectamine LTX (Invitrogen, Carlsbad, CA, USA) according to the manufacturer's instructions, and pre-incubated for 24 hours followed by incubation under hypoxia.

Growth Curve Evaluation

To examine the cell growth, HCC cell lines were plated in triplicate at a density of 5 x 10⁵ cells per dish in 6-cm culture dishes. At the indicated time points after plating, cells were trypsinized, stained with Trypan blue and the number of viable cells were directly scored using a hemocytometer.

Quantification of Intracellular ATP

Total cellular ATP concentration was quantitated using an ATP Detection Reagent kit

(Toyo-ink, Tokyo, Japan). Briefly, pellets of HCC cell lines were homogenized in Tris buffer (25 mmol/L Tris-HCl and 5 mmol/L EDTA, pH 8.0) containing 10% ATP releasing reagent. ATP concentration was determined in a buffer containing 25 mmol/L HEPES, 10 mmol/L MgCl₂, 0.02% sodium azide (pH 7.75), by luciferase bioluminescence detection reagent, according to the manufacturer's instructions.²⁵

Cytofluorimetric Analysis of $\Delta\Psi_m$ and Mitochondrial Structure

Cytofluorimetric analysis of $\Delta\Psi_m$ was performed as previously described.²⁶ Briefly, variations of the mitochondrial transmembrane potential $\Delta\Psi_m$ during hypoxia were also analyzed with 5,5',6,6'-tetrachloro-1,1',3,3'-tetraethylbenzimidazolcarbocyanine iodide (JC-1; Molecular Probes, Eugene, OR, USA). 2.5×10^5 cells were incubated in 100 μ L of PBS containing 0.1 μ M of JC-1 for 30 min. For the FACScan acquisition, the PMT values were 524V and 429V, respectively, for FL1 and FL2; FL1-FL2 compensation was 3% and FL2-FL1 compensation was 21%.

Alteration of mitochondrial structure during hypoxia was analyzed using CellLight Mitochondria-RPF (Invitrogen, Carlsbad, CA, USA), a BacMam expression vectors encoding RPF fused to the leader sequence of E1 α pyruvate dehydrogenase.²⁷ The BacMam technology is based on double-stranded DNA insect viruses, baculoviruses, as vehicles to efficiently deliver and express genes in mammalian cells. Cells were incubated with 50 MOI of this reagent for 30 min and analyzed using immunofluorescence following washing with PBS.

Measurement of β -hydroxybutyrate

β -hydroxybutyrate concentration in cell lysates was spectrophotometrically assayed by modified enzymatic method kit (Abnova, Neihu, Taiwan). Briefly, β -hydroxybutyrate Dehydrogenase was utilized to generate a product, which reacts with the colorimetric probe with an absorbance band at 450 nm. The ratio of β -hydroxybutyrate to protein weight was

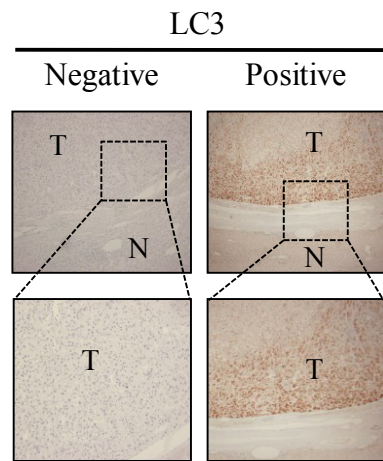
calculated, according to the manufacturer's instructions.²⁸

Statistical Analysis

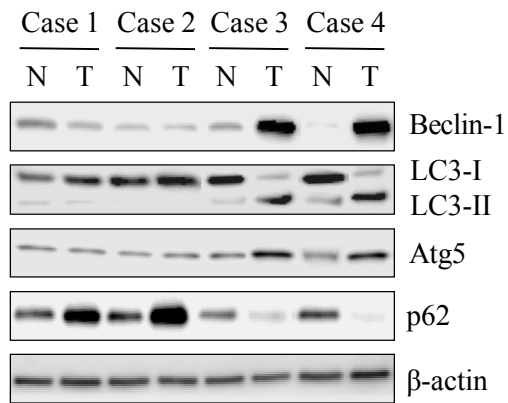
All statistical analyses were performed using JMP statistical software version 7.01 (SAS Institute Inc., Cary, NC, USA). All experiments were independently performed three times in triplicate. All variables are expressed as the mean \pm standard deviation (SD). Continuous variables were compared with independent samples using the nonparametric Wilcoxon test or with dependent samples using the parametric paired t-test. Categorical data were compared using Fisher's test and the chi-squared test. Univariate survival analysis was performed using the Kaplan-Meier method, and the results were compared statistically using the univariate log-rank and Wilcoxon tests. Multivariate analysis was performed using Cox's proportional hazard regression model to evaluate the independent predictive factors of HCC recurrence. P values of < 0.05 were considered significant.

Figure 1

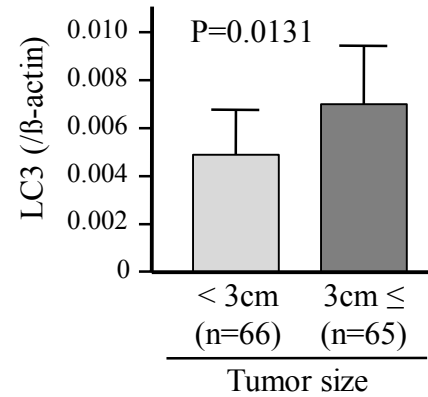
A



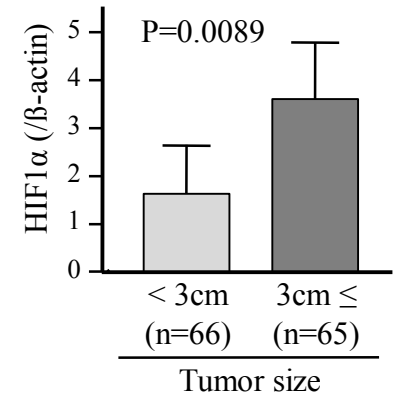
B



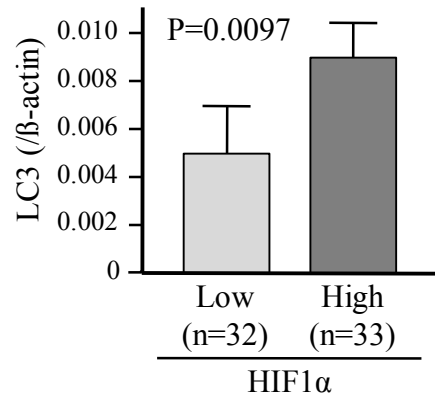
C



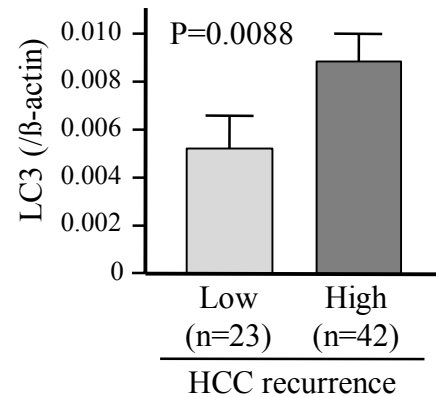
D



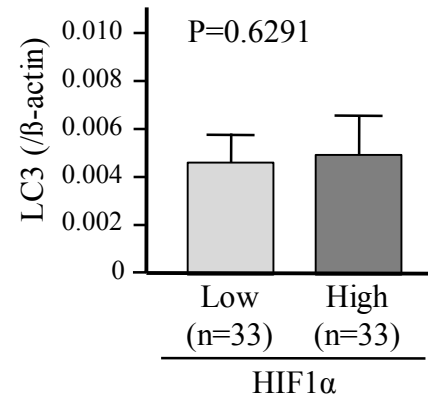
E



F



G



H

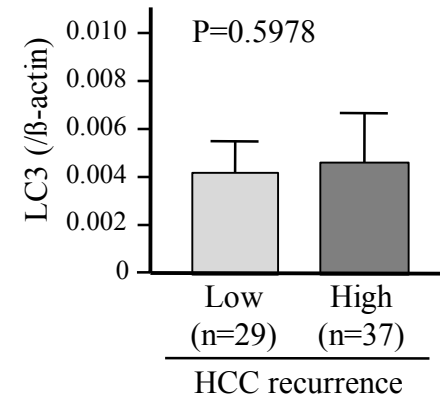
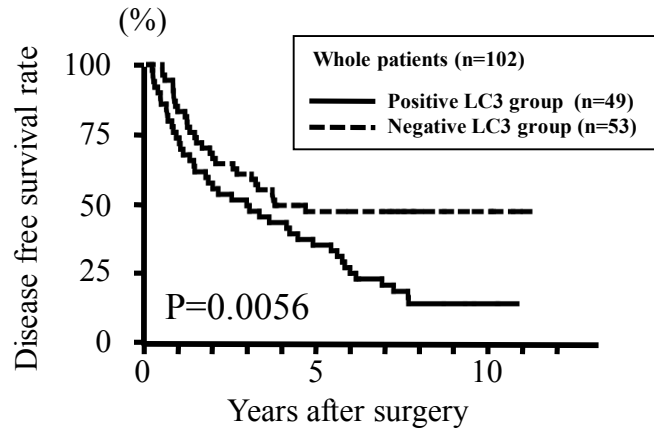
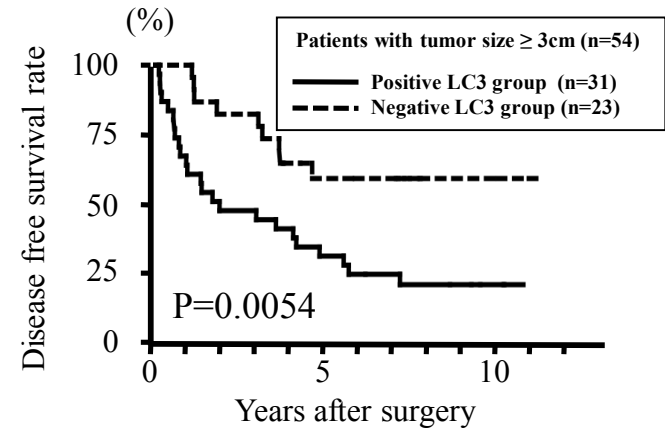


Figure 2

A



B



C

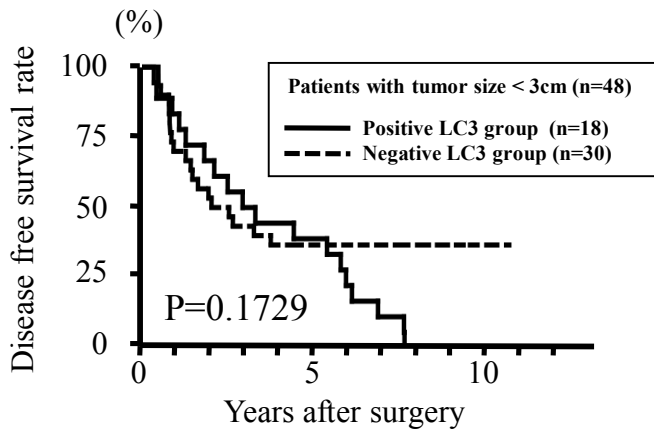
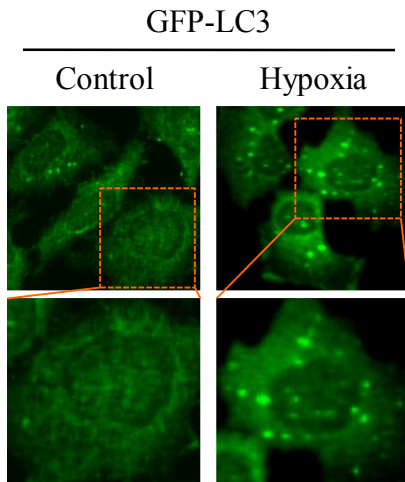
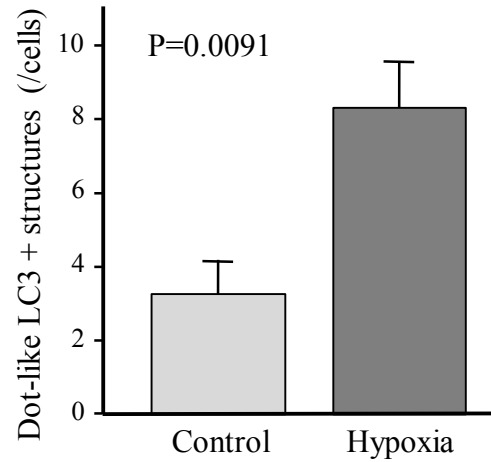


Figure 3

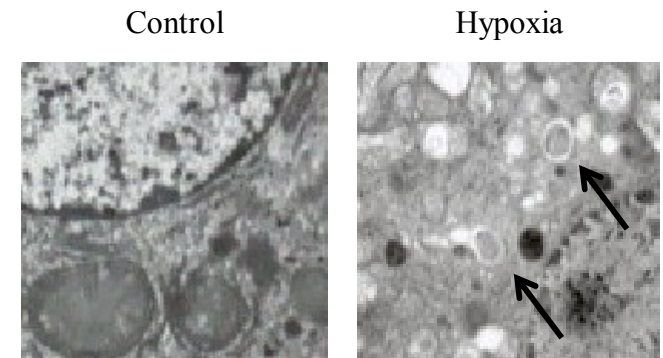
A



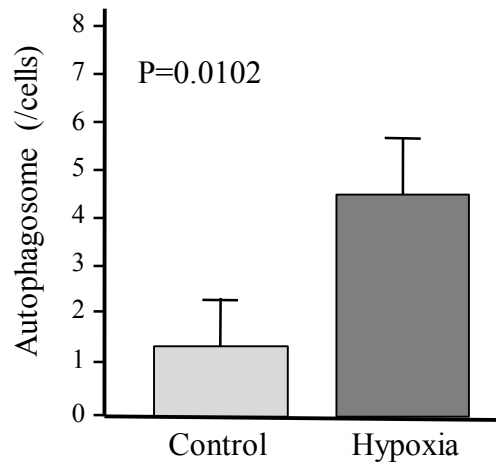
B



C



D



E

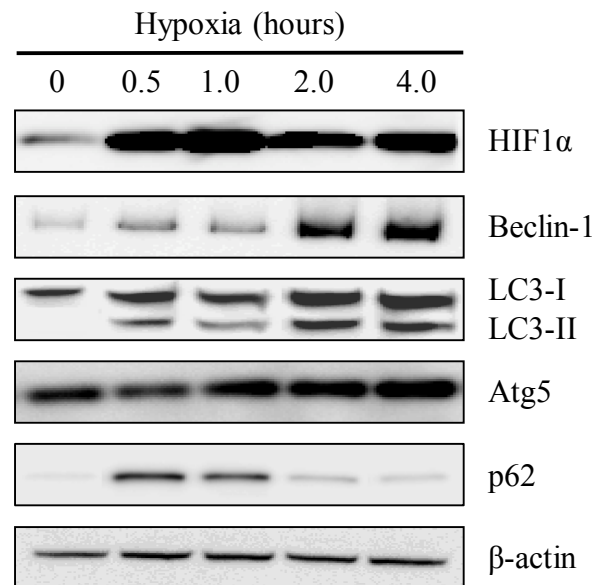


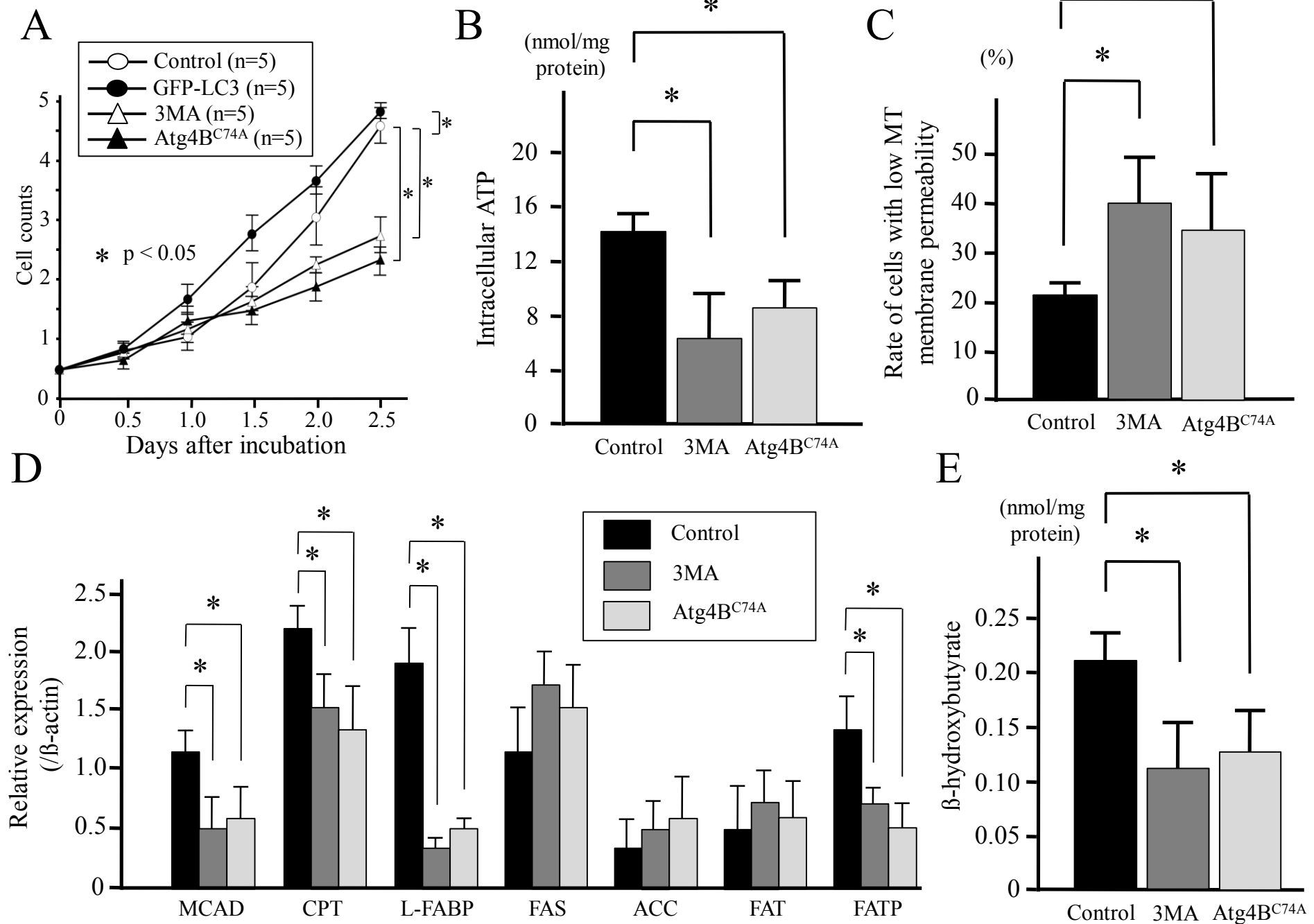
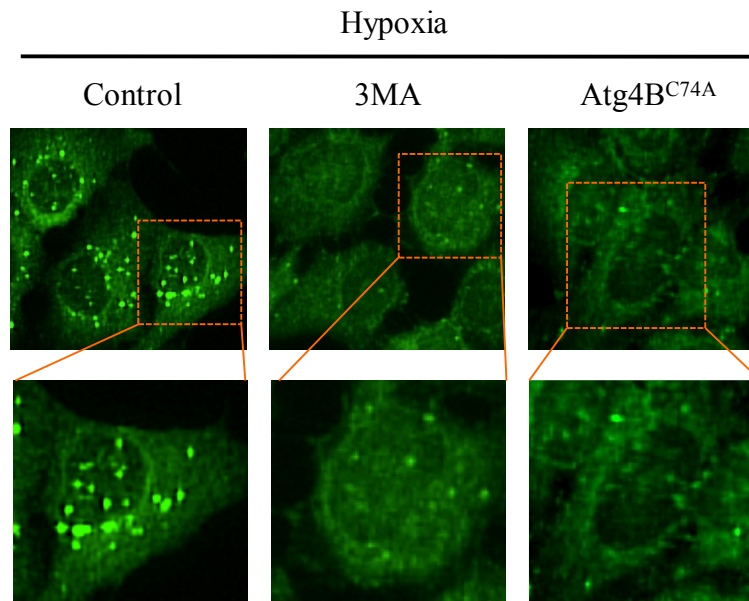
Figure 4

Figure S1

A



B

